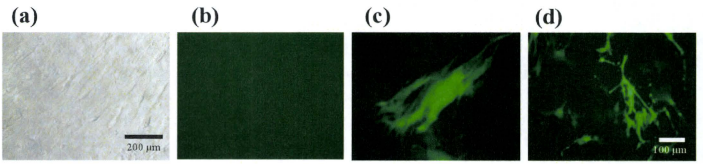

FIGURE 5. Microscopy after GFP gene transfer. (a) Light microscopy of a normal control sample without sonoporation and GFP gene transfer (60 μg/ml). (b) Fluorescent microscopy of a normal control sample without GFP expression. (c, d) Fluorescent microscopy revealed GFP expression after sonoporation with the GFP gene (60 μg/ml) and 10% sonazoid. Scale bar, 100-200 μm.

CONCLUSIONS

This study assessed the gene transfer efficiency of sonoporation in mouse ASCs. Although approximately 40% of the cells were no longer viable after sonoporation, gene transfer to the remaining cells was observed. However, the efficiency of gene transfer was relatively low. It is therefore necessary to improve gene transfer conditions (ultrasound conditions, microbubbles, DNA concentration, etc) in order to improve the gene transfer efficiency of this procedure.

ACKNOWLEDGMENTS

We thank Ms. Rina Yokota (Nagoya University) for her valuable assistance. This work was supported in part by Health and Labor Sciences Research Grants from the Ministry of Health, Labor and Welfare (Tokyo, Japan).

REFERENCES

1. J. M. Gimble, A. J. Katz, and B. A. Bunnell, *Circ Res.* **100(9)**, 1249-1260 (2007).
2. Y. Miyamoto, K. Oishi, H. Yukawa, H. Noguchi, M. Sasaki, H. Iwata and S. Hayashi, *Cell Transplant.* accept.
3. H. Yukawa, H. Noguchi, K. Oishi, M. Inoue, M. Hasegawa, M. Hamaguchi, N. Hamajima and S. Hayashi, *Cell Transplant.* **18(5)**, 601-609 (2009).
4. K. Tachibana, *Hum Cell.* **17(1)**, 7-15 (2004).
5. D. L. Miller, M. A. Averkiou, A. A. Brayman, E. C. Everbach, C. K. Holland, J. H. Wible Jr and J. Wu, *J Ultrasound Med.* **27(4)**, 611-632 (2008).
6. M. Ono, Y. Aratani, I. Kitagawa and Y. Kitagawa, *Exp. Cell Res.* **187**, 309–314 (1990).

Cell Transplantation, Vol. 19, pp. 701–706, 2010
Printed in the USA.

0963-6897/10 $90.00 + .00
DOI: 10.3727/096368910X508799
E-ISSN 1555-3892
www.cognizantcommunication.com

An Improvement in the Attaching Capability of Cryopreserved Human Hepatocytes by a Proteinaceous High Molecule, Sericin, in the Serum-Free Solution

Yoshitaka Miyamoto,*[1] Naozumi Teramoto,† Shuji Hayashi,‡ and Shin Enosawa*

*Clinical Research Center, National Center for Child Health and Development, Tokyo, Japan
†Department of Life and Environmental Sciences, Faculty of Engineering, Chiba Institute of Technology, Chiba, Japan
‡Department of Advanced Medicine in Biotechnology and Robotics, Nagoya University Graduate School of Medicine, Nagoya, Japan

The methodology of cryopreservation of human hepatocytes remains unsatisfactory. Even when the viability of thawed cells is tolerable, the cells often lose the attaching capability to a culture dish, resulting in the cells' inability to survive. Previously, we described the effectiveness of maltose on the attachment of hepatocytes. This article demonstrates that a silk-derived high molecular protein, sericin, improves the cell-attaching capability in the serum-free freezing medium. When human hepatocytes [initial viability: 60.9 ± 3.1% (mean ± SD, $n = 3$)] were frozen with serum-free Dulbecco's modified Eagle medium (DMEM) containing 10% dimethyl sulfoxide (DMSO), the viability was 29.4 ± 3.2% and the cell-attaching capability 20.4 ± 4.1%. On the other hand, DMEM containing 10% DMSO and 1% sericin increased the values to 45.0 ± 0.8% and 26.2 ± 3.2%. Moreover, the addition of 0.1 mol/L maltose to the sericin-containing medium improved to 42.2 ± 3.2% and 51.1 ± 1.0%, as we demonstrated in a previous report. The present results indicated that sericin combined with maltose is a novel additive in the serum-free freezing medium for human hepatocytes.

Key words: Cryopreservation; Human hepatocytes; Sericin

INTRODUCTION

An improvement in the cryopreservation of hepatocytes is expected to greatly benefit not only the research field but also the clinical cell transplantation field. The present major requirement is that pharmaceutical companies use human hepatocytes for predicting the metabolism of drug candidates (2). The potential demand will be elevated in clinical cell transplantation and the bioartificial liver. The number of cases of hepatocyte transplantation is gradually increasing, and in some cases the cells were transplanted repeatedly from the same donor to confirm effectiveness (5). Consequently, a reliable cryopreservation protocol needs to be established. However, hepatocytes easily lose their cell viability after cryopreservation.

We noticed that the cell viability immediately after thawing does not reflect the cells' survival in the culture condition. Therefore, we have been trying to improve cell survival by a modification of the freezing medium. Previously, we reported the different efficacies of oligosaccharides on the attachment capability of cryopreserved hepatocytes and arrived at the conclusion that maltose is the most effective additive (6), while trehalose, which belongs to the same dissacharide as maltose, is thought to be effective elsewhere (3,4). Therefore, we embarked on the development of a serum-free freezing solution to ensure the safety of cells for clinical transplantation, especially to avoid xenozoonoses.

Sericin is a silk-derived high molecular protein and was reported recently to be useful for cell cryopreservation (7), but the effectiveness for cryopreservation of primary hepatocytes has not been tested. Here we demonstrate that sericin can replace serum in the freezing solution, and that the addition of maltose resulted in a marked improvement in the cell-attaching capability after thawing.

MATERIALS AND METHODS

Materials

The materials used in the present study were obtained as follows. Dulbecco's modified Eagle medium (DMEM),

Received June 1, 2009; final acceptance April 21, 2010. Online prepub date: June 3, 2010.
[1]Present address: Department of Advanced Medicine in Biotechnology and Robotics, Nagoya University Graduate School of Medicine, Nagoya 466-8550, Japan.
Address correspondence to Shin Enosawa, Clinical Research Center, National Center for Child Health and Development, 2-10-1 Ookura, Setagaya-ku, Tokyo 157-8535, Japan. Tel: +81-3-3416-0181; Fax: +81-3-3417-2864; E-mail: senosawa@nch.go.jp

Williams medium E, and antibiotics (penicillin, streptomycin, and kanamycin) were from GIBCO BRL, Life Technologies (Grand Island, NY). Fetal bovine serum (FBS) was produced from Gemini Bio-Products (West Sacramento, CA). Insulin, dexamethasone, and dimethyl sulfoxide (DMSO, D-2650) were purchased from Sigma-Aldrich (St. Louis, MO). Maltose was obtained from Wako Pure Chemical Industries, Ltd. (Osaka, Japan). A Live/Dead Viability Cytotoxicity Kit (L3224) was obtained from Molecular Probes (Eugene, OR). All other materials and chemicals not specified above were of the highest grade. Sericin hydrolysate with an average molecular mass of 30 kDa was generously supplied from Seiren Co. Ltd. (Fukui, Japan).

Procurement of Human Primary Hepatocytes

Human hepatocytes were isolated from the nontransplantable livers of three different donors (age/race/sex/cold ischemia time: 34/African-American/female/38 h; 36/Caucasian/male/30 h; 57/Asian/male/27 h) originally procured by the National Disease Research Interchange (NDRI) in Philadelphia (USA), and imported by the Human and Animal Bridging Research (HAB) Organization (Chiba, Japan). The cell isolation was performed by a collagenase perfusion method as described previously (6).

Hepatocyte Freezing and Thawing Procedures

The basic composition of the cryopreservation medium was DMEM containing 100 U/ml penicillin, 100 U/ml streptomycin, and 10% DMSO. Maltose was added to this medium at concentrations of 0.1 mol/L and sericin at 1%. One milliliter of cell suspension containing 5×10^6 cells was quickly transferred to a 2.0-ml freezing tube and placed in a controlled rate freezer (Kryo10, Planer, Middlesex, UK). The freezing protocol was described previously (6). Immediately after freezing, the tubes were transferred to liquid nitrogen and stored for 1–3 months. In order to thaw cells, the tubes were placed in a 37°C water bath for 90 s. The cell suspension was then diluted one- to ninefold with ice-cold DMEM. The suspension was centrifuged for 1 min at $50 \times g$. After the supernatant was removed, the cells were resuspended in fresh medium and the cell viability was assessed by a trypan blue exclusion test. The final concentration of trypan blue (GIBCO BRL) was 0.2%.

Hepatocyte Culture and Determination of Cell Survival

Freshly isolated or cryopreserved/thawed hepatocytes (4×10^5 live cells) were seeded into 35-mm collagen-coated dishes (Biocoat Cellware, Bedford, MA) in 2 ml of Williams medium E containing 10% FBS, 1 μmol/L insulin, 1 μmol/l dexamethasone, 100 μg/ml kanamycin, 100 U/ml penicillin, and 100 U/ml streptomycin. The cells were incubated at 37°C under a humidified 5% CO_2 atmosphere. The culture medium was changed at 6 and 24 h after seeding. The cell survival rates were estimated by microscopic observation of the attached cells 24 h after seeding, using the NIH IMAGE program (National Institutes of Health, http://rsb.info.nih.gov/nih-image/). Two fields in each well of three wells (total six fields) were examined and the average was calculated. In order to confirm the viability of cultured cells, hepatocytes were stained with calcein and ethidium bromide (Live/Dead Viability/Cytotoxicity Kit).

Osmolality Measurements and Differential Scanning Calorimetry (DSC) Analysis

The osmolality of freezing medium was measured using a Vapor Pressure Osmometer (VAPRO 5520, Wescor, USA). Differential scanning calorimetry (DSC) was performed by a Perkin Elmer differential scanning calorimeter, Diamond DSC, under a helium atmosphere using a cooling attachment with liquid nitrogen. For the measurement, 5 μl of the sample was taken into a small aluminum pan. The temperature of the sample was changed according to the same programmed schedule as was used for the hepatocyte cryopreservation.

Ethical Consideration

All experimental procedures using human hepatocytes were performed after permission from the institutional review board of National Center for Child Health and Development.

RESULTS

Survival of Human Hepatocytes Cryopreserved Under Different Conditions

The representative microscopic appearances of the cultured hepatocytes from a 34-year-old African-American female are shown in Figure 1. Almost all attached cells had transparent cytoplasm with a firm smooth surface. Because the culture medium was aspirated and plated, washed extensively, and supplied with fresh medium at 6 h after inoculation, there were few dead cells attached to the plate except for small-sized round nuclei. In fact, when cells were stained with calcein and ethidium bromide, all cells are calsein-positive live cells and only the small, probably naked nuclei were stained red by ethidium bromide (Fig. 1K). It was apparent that the cells cryopreserved in DMEM-containing DMSO and maltose (Fig. 1D), and containing DMSO, maltose, and sericin (Fig. 1G) attached well onto the culture plate and that these cells had a better appearance than that of the freshly isolated hepatocytes (Fig. 1A). The attachment of cells stored in DMEM-containing DMSO and sericin (Fig. 1E) was slightly better than the attachment of the cells stored in DMEM containing DMSO only (Fig. 1B), containing DMSO and FBS (Fig. 1C), and containing

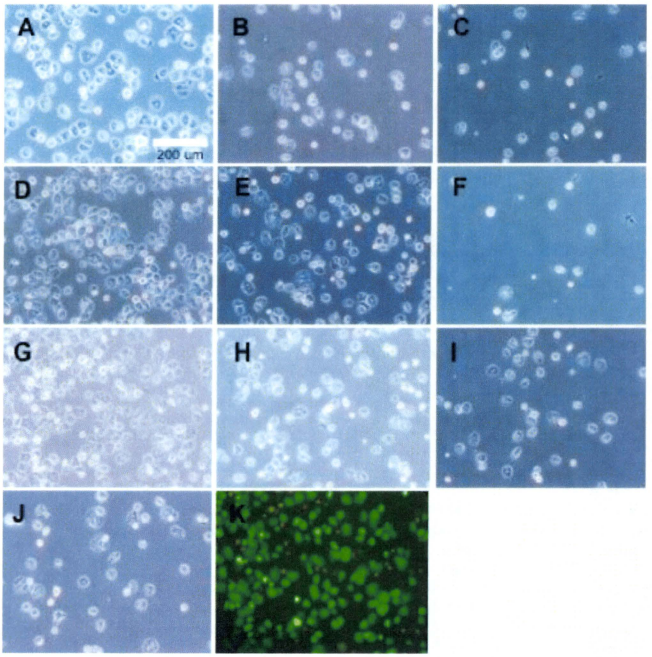

Figure 1. The phase-contrast photomicrographs of human hepatocytes before (A) and after the cryopreservation (B–G). The hepatocytes were cultured on type I collagen cell culture dish for 24 h after the inoculation. Scale bar: 200 μm. The hepatocytes were cryopreserved with DMEM containing 10% DMSO (base medium) (B), base medium + 10% FBS (C), base medium + 0.1 mol/L maltose (D), base medium + 1% sericin (E), base medium + 10% FBS, 1% sericin (F), base medium + 0.1 mol/L maltose, 1% sericin (G), base medium + 10% FBS, 0.1 mol/L maltose (H), base medium + 10%FBS, 0.1mol/L maltose, 1% sericin (I), Cell Banker 1 (J). (K) Fluorescent photomicrograph of (G) after staining with calcein and ethidium.

DMSO, FBS, and maltose (Fig. 1H). In contrast, the combination of FBS and sericin did not appear favorable for the cryopreservation (Fig. 1F, I). The cell attachment after storage by a commercially available cryopreservant, Cell Banker 1 (Fig. 1J) was the same as that for DMEM-containing DMSO and FBS (Fig. 1B).

Quantitative Evaluation of Cell Viability and Cell-Attaching Capability

In order to quantify the morphological differences, we determined the cell viability immediately after thawing and the cell-attaching capability (Fig. 2A and B, respectively). The values of the two indices are of independent nature, one from numbers of viable and total cells and the other from an occupied area in the microscopic field. The initial viability of freshly isolated hepatocytes was 61 ± 3.1% (condition 1, average ± SD, n = 3). The viability of cells cryopreserved in DMEM-containing DMSO only was 29 ± 3.2% and cell attachment was 20.4 ± 4.1%. When we used the other control, Cell Banker 1, the cell viability was reasonably good (46.0 ± 1.1%), but the cell attachment capability was quite low (13.4 ± 1.5%). This type of discrepancy between the initial cell viability and cell survival was often observed with the cryopreserved hepatocytes. The addition of FBS did not improve the cell viability (condition 3, 30.2 ±

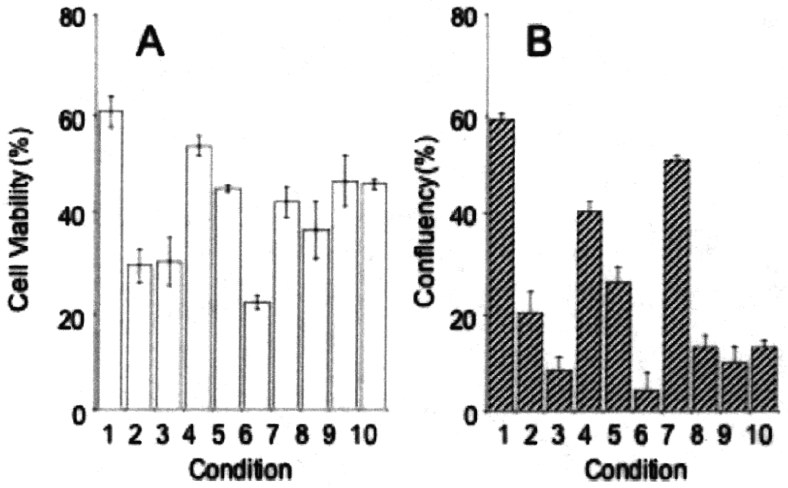

Figure 2. Cell viability (A) and attaching capability (B) of cryopreserved human hepatocytes with a different composition of the preservation solution. 1: Freshly isolated hepatocytes; 2: DMEM containing 10% DMSO (base medium); 3: base medium + 10% FBS; 4: base medium + 0.1 mol/L maltose; 5: base medium + 1% sericin; 6: base medium + 10% FBS, 1% sericin; 7: base medium + 0.1 mol/L maltose, 1% sericin; 8: base medium + 10% FBS, 0.1 mol/L maltose; 9: base medium + 10% FBS, 0.1 mol/L maltose, 1% sericin; 10: Cell Banker 1. The data are the means and SD of three independent experiments.

4.7%), but maltose (condition 4, viability: 54.0 ± 2.1%, attaching capability: 40.2 ± 2.2%) and sericin (condition 5, viability: 45.0 ± 0.8%, attaching capability: 26.2 ± 3.2%) increased both the cell viability and attaching capability. The most marked effect was observed with DMEM-containing DMSO, maltose, and sericin (condition 7, viability: 42.2 ± 3.2%, attaching capability: 51.0 ± 1.0%). As expected from the morphological observation (Fig. 1), the combination of sericin and FBS decreased both the cell viability and attaching capability (condition 6), while the addition of maltose resulted in more favorable values for the corresponding controls (conditions 8 and 9).

Comparison of Physical Characteristics of Freezing Solutions

The osmolality of the freezing solution is listed in Table 1. The value of DMEM culture medium was 0.312 mol/kg, almost equal to that of typical isotonic solutions (0.28–0.29 mol/kg, data not shown). When DMSO was added, the value increased to 1.922 but no marked elevation occurred by the addition of FBS, maltose, or sericin. Figure 3 shows the DSC analysis of the effect of maltose and sericin in the freezing solution. The spike indicates the starting point of crystallization. Each additive affected the crystallization temperature. Interestingly, the solution containing both sericin and maltose showed crystallization at the earlier phases containing sericin or maltose only. However, no obvious relationships were observed between the cell biological protecting activity and the physical parameters this time.

DISCUSSION

A lot of factors have been proposed to cause cell damage by cryopreservation, such as ice crystal formation, condensation of salts the free water, dehydration, etc. (8). After laborious efforts by numerous researchers, DMSO has emerged as one of the major cryoprotective agent for cells. However, DMSO itself does not sufficiently protect the cell from damage during the cryopreservation process. We previously reported that the addition of maltose to DMSO-based serum containing cryopreservation medium improved the cell-attaching capability of hepatocytes (6). In this report, we demon-

Table 1. Osmolality of Various Freezing Media Used for Human Hepatocytes

Composition	Osmolality (mol/kg)
1. DMEM only	0.312
2. DMEM, 10% DMSO	1.922
3. DMEM, 10% DMSO, 10% FBS	1.965
4. DMEM, 10% DMSO, 0.1 mol/L maltose	1.943
5. DMEM, 10% DMSO, 1% sericin	1.963
6. DMEM, 10% DMSO, 0.1 mol/L maltose, 1% sericin	1.978

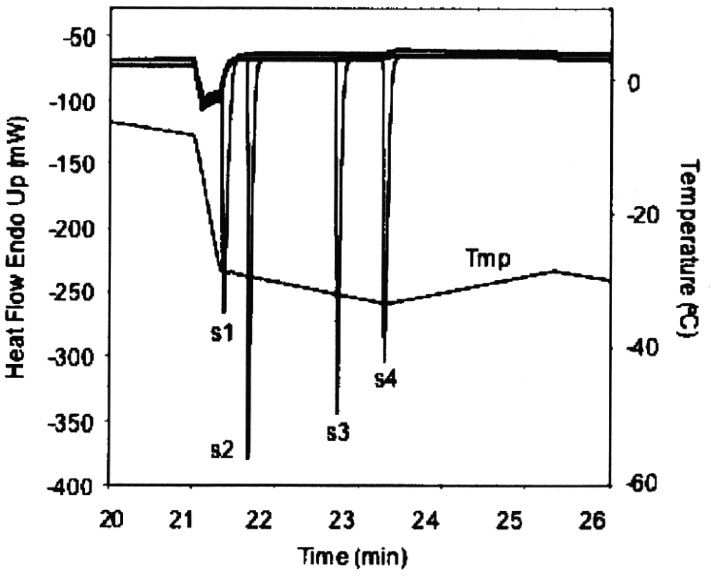

Figure 3. The effect of the additives in the freezing media by differential scanning calorimetry (DSC) analysis. s(spike)1: DMEM containing 10% DMSO (base medium); s2: base medium + 0.1 mol/L maltose, 1% sericin; s3: base medium + 1% sericin; s4: base medium + 0.1 mol/L maltose. Tmp indicates the temperature of the test medium. The solution temperature of each spike: s1: −28.0°C, s2: −29.1°C, s3: −31.8°C, s4: −32.5°C.

strated that silk origin protein, sericin, can replace serum in the medium.

The advantage of serum-free medium is not merely the avoidance of xenozoonoses, but the emergence of quality differences of the serum lots. Sericin is a protein hydrolysate from raw silk and it is rich in serine (an average molecular weight of 30 kDa). Recently, sericin was reported as a novel cryopreservation agent of mammalian and insect cell lines (7). We expanded the utility of sericin to primary hepatocytes, cells that are perhaps the most difficult to storevia freezing. Because of the advantages described above, sericin-containing medium may become one option for the clinical transplantation of cryopreserved hepatocytes.

Ice crystal formation is likely to be a major hurdle to succeed cryopreservation. DSC measurement is often used to study ice formation in the multicomponent liquid phase (1). Unfortunately, no meaningful relationship between cell biological assessment and DSC as well as osmolality was gleaned from the present results, but the diligence of these physical approaches should be conducted in conjunction with biological evaluations.

ACKNOWLEDGMENTS: Firstly, we would like to express deep gratitude to the persons who donated the livers for research and to their family members. We also thank Dr. Satoshi Suzuki of HAB Research Organization, Japan for supplying the human hepatocytes and Seiren Co. Ltd., Fukui, Japan for the generous gift of sericin. This research was supported by Grant-in-aid (KH71066 and KHD1027) from the Japan Health Sciences Foundation, Tokyo, Japan and by the Sasakawa Scientific Research Grant from The Japan Science Society.

REFERENCES

1. Bryant, G. DSC measurement of cell suspensions during successive freezing runs: Implications for the mechanisms of intracellular ice formation. Cryobiology 32:114–128; 1995.
2. Hewitt, N. J.; Lech, M. J.; Houston, J. B.; Hallifax, D.; Brown, H. S.; Maurel, P.; Kenna, J. G.; Gustavsson, L.; Lohmann, C.; Skonberg, C.; Guillouzo, A.; Tuschl, G.; Li, A. P.; LeCluyse, E.; Groothuis, G. M.; Hengstler, J. G. Primary hepatocytes: current understanding of the regulation of metabolic enzymes and transporter proteins, and pharmaceutical practice for the use of hepatocytes in metabolism, enzyme induction, transporter, clearance, and hepatotoxicity studies. Drug Metab. Rev. 39:159–234; 2007.
3. Illouz, S.; Nakamura, T.; Webb, M.; Thava, B.; Bikchandani, J.; Robertson, G.; Lloyd, D.; Berry, D.; Wada, H.; Dennison, A. Comparison of University of Wisconsin and ET-Kyoto preservation solutions for the cryopreservation of primary human hepatocytes. Transplant. Proc. 40:1706–1709; 2008.
4. Katenz, E.; Vondran, F. W.; Schwartlander, R.; Pless, G.; Gong, X.; Cheng, X.; Neuhaus, P.; Sauer, I. M. Cryopreservation of primary human hepatocytes: the benefit of trehalose as an additional cryoprotective agent. Liver Transpl. 13:38–45; 2007.
5. Lee, K. W.; Lee, J. H.; Shin, S. W.; Kim, S. J.; Joh, J. W.; Lee, D. H.; Kim, J. W.; Park, H. Y.; Lee, S. Y.; Lee,

H. H.; Park, J. W.; Kim, S. Y.; Yoon, H. H.; Jung, D. H.; Choe, Y. H.; Lee, S. K. Hepatocyte transplantation for glycogen storage disease type Ib. Cell Transplant. 16:629–637; 2007.
6. Miyamoto, Y.; Suzuki, S.; Nomura, K.; Enosawa, S. Improvement of hepatocyte viability after cryopreservation by supplementation of long-chain oligosaccharide in the freezing medium in rats and humans. Cell Transplant. 15:911–919; 2006.
7. Sasaki, M.; Kato, Y.; Yamada, H.; Terada, S. Development of a novel serum-free freezing medium for mammalian cells using the silk protein sericin. Biotechnol. Appl. Biochem. 42:183–188; 2005.
8. Terry, C.; Dhawan, A.; Mitry, R. R.; Hughes, R. D. Cryopreservation of isolated human hepatocytes for transplantation: State of the art. Cryobiology 53:149–159; 2006.

Biomaterials 31 (2010) 4094–4103

Contents lists available at ScienceDirect

Biomaterials

journal homepage: www.elsevier.com/locate/biomaterials

Quantum dots labeling using octa-arginine peptides for imaging of adipose tissue-derived stem cells

Hiroshi Yukawa [a,*], Yukimasa Kagami [b], Masaki Watanabe [b], Koichi Oishi [a], Yoshitaka Miyamoto [a], Yukihiro Okamoto [b,c], Manabu Tokeshi [b,c], Noritada Kaji [b], Hirofumi Noguchi [d], Kenji Ono [e], Makoto Sawada [e], Yoshinobu Baba [b,c,f,g,h], Nobuyuki Hamajima [i], Shuji Hayashi [a]

[a] Department of Advanced Medicine in Biotechnology and Robotics, Nagoya University Graduate School of Medicine, Nagoya University, Higashi-ku, Nagoya 461-0047, Japan
[b] Department of Applied Chemistry, Nagoya University Graduate School of Engineering, Nagoya University, Furo-cho, Chikusa-ku, Nagoya 464-8603, Japan
[c] MEXT Innovative Research Center for Preventive Medical Engineering, Nagoya University, Furo-cho, Chikusa-ku, Nagoya 464-8603, Japan
[d] Baylor Institute for Immunology Research, Baylor Research Institute, 3434 Live Oak St., Dallas, TX 75204, USA
[e] Research Institute of Environmental Medicine, Stress Adaption and Protection, Nagoya University, Furo-cho, Chikusa-ku, Nagoya, 464-8601, Japan
[f] Plasma Nanotechnology Research Center, Nagoya University, Furo-cho, Chikusa-ku, Nagoya 464-8603, Japan
[g] Health Technology Research Center, National Institute of Advanced Industrial Science and Technology (AIST), Hayashi-cho 2217-14, Takamatsu 761-0395, Japan
[h] Institute for Molecular Science, National Institutes of Natural Sciences, Myodaiji Nishigo-naka 38, Okazaki 444-8585, Japan
[i] Department of Preventive Medicine, Biostatistics and Medical Decision Making, Nagoya University Graduate School of Medicine, Nagoya 466-8550, Japan

ARTICLE INFO

Article history:
Received 30 October 2009
Accepted 27 January 2010
Available online 19 February 2010

Keywords:
Semiconductor
Quantum dots (QDs)
Cell-penetrating peptides (CPPs)
In vivo imaging
Adipose tissue-derived stem cells (ASCs)

ABSTRACT

Quantum dots (QDs) have been used to study the effects of fluorescent probes for biomolecules and cell imaging. Adipose tissue-derived stem cells, which carry a relatively lower donor site morbidity, while yielding a large number of stem cells at harvest, were transduced with QDs using the octa-arginine peptide (R8) cell-penetrating peptide (CPP). The concentration ratio of QDs:R8 of 1×10^4 was optimal for delivery into ASCs. No cytotoxicity was observed in ASCs transduced with less than 16 nM of QDs655. In addition, >80% of the cells could be labeled within 1 h and the fluorescent intensity was maintained at least for 2 weeks. The ASCs transduced with QDs using R8 could be differentiated into both adipogenic and osteogenic cells, thus suggesting that the cells maintained their stem cell potency. The ASCs labeled with QDs using R8 were further transplanted subcutaneously into the backs of mice or into mice through the tail vein. The labeled ASCs could be imaged with good contrast using the Maestro *in vivo* imaging system. These data suggested that QD labeling using R8 could be utilized for the imaging of ASCs.

1. Introduction

Quantum dots (QDs) are inorganic probes that consist of CdSe/ZnS-core/shell semiconductor nanocrystals. QDs have several distinctive advantages in comparison to conventional organic labels such as a high luminance, resistance to photobleaching (long time labeling), a range of excitation wavelengths and narrower emission bandwidths [1–4]. According to these characteristics, QDs have recently been investigated as fluorescent probes for biomolecules and live cells, and are expected to be used in medical applications for diagnostics [5,6]. Various approaches have been applied to label cells with QDs, such as microinjection, electroporation, liposome-based transduction and special peptide delivery [7–11].

The transduction of QDs into cells using cell-penetrating peptides (CPPs) has been established and is thought to a useful technique because of the low cytotoxicity and high transduction efficiency. Yun Lei et al. showed that Tat peptide conjugated QDs could be transduced into mesenchymal stem cells [12]. Jui-Chih Chang et al. showed that Pep-1 labeled QDs could be transduced into stem cells and remained for about one month [13]. However, few detailed studies have so far explored the appropriate ratio of QDs and peptide, uptake time, cell function *in vitro* and application of *in vivo* imaging.

Regenerative medicine is expected to overcome the shortage of donated organs, donor site morbidity and immune reaction [14]. Many kinds of stem cells have been discovered already and provided numerous applications in regenerative medicine. Mesenchymal stem cells (MSCs) and progenitor cells are detected in various tissues, including umbilical cord blood, bone marrow, periodontal ligament and adipose tissue.

Bone marrow-derived stem cells (BMSCs) have the ability to differentiate into multiple mesenchymal cells such as cardiomyocytes, chondrocytes, osteoblasts and adipocytes.

* Corresponding author. Tel.: +81 52 719 1975; fax: +81 52 719 1977.
E-mail address: hiroshiy@med.nagoya-u.ac.jp (H. Yukawa).

0142-9612/$ – see front matter © 2010 Elsevier Ltd. All rights reserved.
doi:10.1016/j.biomaterials.2010.01.134

Therefore, BMSCs have been considered to be an important source of stem cells for use in regenerative medicine.

Recently, adipose tissue-derived stem cells (ASCs) have been increasingly recognized as multipotent stem cells and as an alternative source of BMSCs [15]. ASCs are easier to obtain in abundance by minimally invasive harvest procedures such as lipoaspiration with local anesthesia. In addition, ASCs possess the ability of self-renewing and differentiating into various mesenchymal cell types, while also secreting significant levels of many potent growth factors and cytokines, such as vascular endothelial growth factor (VEGF) and hepatocyte growth factor (HGF) [16]. Because of their potential clinical application, it has therefore become important to label the cells for tracing as transplanted cells.

Previous studies have shown that a cationic liposome (Lipofectamine) could transduce negatively charged QDs into ASCs within 4 h and the QDs remained in the cells for more than 2 weeks. However, cytotoxicity was observed at a relatively low concentration, suggesting that the major cause was the liposome (Lipofectamine) [17]. In this study, octa-arginine peptide (R8), which exhibits even greater efficiency in the delivery of several proteins, was utilized as a delivery vector and the characteristics of negatively charged carboxyl QDs transduced using R8 to live ASCs were investigated. In addition, imaging studies in subcutaneous transplantation on the back and intravenous transplantation through the tail vain were conducted.

2. Materials and methods

2.1. Animals

C57BL/6 mice were purchased from SLC Japan. The mice were housed in a controlled environment (12 h light/dark cycles at 21 °C) with free access to water and a standard chow diet before sacrifice. All conditions and handing of animals in this study were conducted with protocols approved by the Nagoya University Committee on Animal Use and Care.

2.2. Isolation and culture of ASCs

The 7–14-month-old female C57BL/6 mice were killed by cervical dislocation; adipose tissue specimens in the inguinal groove were isolated and washed extensively with Hank's balanced salt solution or phosphate-buffered saline (PBS) to remove the blood cells. The isolated adipose tissue specimens were cut finely and digested with 1 mL of 1 mg/mL typelcollagenase (Collagenase TypeI, 274 U/mg, Koken Co., Ltd., Tokyo, Japan) at 37 °C in a shaking water bath for 45 min. The cells were filtrated using 250 μm nylon cell strainers (BD Biosciences) and suspended in Dulbecco's modified Eagle's medium and full-length name of F12 (DMEM/F12) containing 20% fetal bovine serum (FBS: Trace Scientific Ltd., Melbourne, Australia, Uin: 53141 Lot: B01249-500) and 100 U/ml penicillin/streptomycin (culture medium). They were centrifuged at 1200 rpm for 5 min at room temperature and adipose tissue-derived stem cells (ASCs) were obtained from the pellet. They were washed three times by suspension and centrifugation in culture medium and then were incubated overnight in culture medium at 37 °C with 5% CO_2. The primary cells were cultured for several days until they reached confluence and were defined as passage "0". The cells were used for the experiments between passages 2 and 5.

2.3. Preparation and transduction of R8-QDs complex

QDs (Invitrogen; Qdot ITK Carboxyl Quantum Dots) and R8 (Sigma genosys, Japan) were purchased. QDs were made from nanometer-scale crystals of a semiconductor material (CdSe), which are shelled with an additional semiconductor layer (ZnS) to improve their chemical and optical properties. In addition, the polymer coating has COO^- surface groups. To determine the optimal concentration ratio of QDs655 (emission at 655 nm)/R8 to transduce into ASCs, QDs655 (2.0 nM) and R8 were mixed for 20 min at room temperature in various ratios of QDs655/R8. Next, ASCs were incubated with the R8-QDs655 complex in a transduction medium (DMEM/F12, 2% FBS, 100 U/mL penicillin/streptomycin) at 37 °C. After 4 h incubation, the transduction efficiency of QDs655 into ASCs was evaluated by conventional fluorescence microscopy and a flow cytometry analysis [18].

2.4. Flow cytometry analysis

ASCs (1.5×10^5 cells) were seeded in 12-well plates (BD Biosciences) with 500 μL of culture medium for 2 h and the cells were transduced with QDs655 using R8 in transduction medium at 37 °C. After transduction, the cells were washed three times by suspension and centrifugation at 1200 rpm for 3 min. Next, the cells were suspended in 500 μL of PBS and used for flow cytometry analysis on a FACS caliber (BD Biosciences) flow cytometer using 488 nm laser excitation and 615 nm long pass emission.

2.5. Cytotoxicity of QDs to ASCs

The cells (2×10^4 cells) were seeded in 96-well plates (BD Biosciences) with 100 μL of culture medium for 2 h and then they were replaced with 100 μL of transduction medium at 37 °C. After 4 h incubation, QDs655 (0–24 nM) and R8 were mixed at the optimal ratio of 1:1 $\times$ 10^4, and ASCs were transduced with QDs655 using R8 in transduction medium for 24 h. Viable cells were counted using Cell Counting Kit-8 (CCK-8; DOJINDO Laboratories Kumamoto, Japan). CCK-8 reagent (10 μL) was added to each well and the reaction was allowed to proceed for up to 4 h. The absorbance of the sample at 450 nm was measured against a background control using a microplate reader.

2.6. Proliferation of ASCs labeled with QDs

ASCs (1×10^3 cells) were seeded in 96-well plate with 100 μL of culture medium and then transduced with QDs655 using R8 at various concentrations of QDs655 for 4 h. Next, the media was replaced with 100 μL of culture medium. After 0, 2, 4 and 5 days, viable cells were counted using the Cell Counting Kit-8 in the same way.

2.7. Confocal laser scanning microscopy

A confocal laser scanning microscopy (FV1000, OLYMPUS) analysis was conducted to confirm the fluorescent intensity and location of QDs655 in labeled ASCs using R8. Images obtained from the bottom of the coverslip to the top of the cells were recorded and each image was superimposed on PC to qualify the total brightness and pixel area of each region of interest. Before imaging, the cells were washed three times with PBS and replaced with fresh transduction medium [19].

2.8. Transduction of QDs using R8

ASCs were preincubated in the transduction medium with 10 mM sodium azide and 2-deoxy-D-glucose (endocytosis inhibitors) for 1 h at 37 °C, or 3 mM amiloride (macropinocytosis inhibitor) for 10 min at 37 °C. In addition, ASCs were preincubated in the transduction medium for 30 min at 4 °C (both endocytosis and macropinocytosis inhibitors). These cells were then washed three times with PBS followed by the addition of 0.4 nM QDs655 with R8 in fresh transduction medium for 1 h. Thereafter, the cells were observed using confocal laser scanning microscopy.

2.9. Adipogenic differentiation

Adipogenic differentiation was induced by culturing the cells for 3 days in DMEM (high glucose) containing 100 μM indometacin, 1 μM dexamethasone, 1 μM hydrocortisone, 10 μM insulin (Sigma, I-5500) and 10% FBS. The cells were then further cultured in DMEM (high glucose) containing 10% FBS for 2 weeks and the medium was changed every 3 days. Differentiation was confirmed by conventional microscopic observations of intracellular lipid droplets and Oil Red O staining as an indicator of intracellular lipid accumulation. Briefly, the cells were fixed in 10% solution of formaldehyde in PBS for at least 10 min at room temperature and then were washed with 60% isopropanol. Next, the cells were stained with 2% (w/v) Oil Red O reagent for 10 min at room temperature followed by repeated washing with distilled water and destaining in 100% isopropanol for 1 min.

2.10. Osteogenic differentiation

Osteogenic differentiation was induced by culturing the cells for 2 weeks in DMEM containing 200 μM dexamethasone, 50 μM ascorbate-2-phosphate (Wako Pure Chemical Industries Ltd., 013-12061), 10 mM α-glycerophosphate (Sigma, G-9891) and 10% FBS. The differentiation was confirmed by staining for any alkaline phosphatase activity and then observing the extracellular matrix calcification using Von Kossa's method. The cells were washed twice with PBS and fixed in 10% formalin for 15 min at room temperature. They were washed and incubated with deionized water for 15 min. Then, they were stained with a solution containing naphtol AS MX-PO_4 (Sigma, N-5000), *N,N*-dimethylformamide (Wako Pure Chemical Industries Ltd.), Red Violet LB salt (Sigma, F-1625) and Tris–HCl buffer (pH 8.3) for 45 min. Von Kossa staining was carried out with 2.5% silver nitrate solution for 30 min.

2.11. RNA extraction and real-time RT-PCR

Total RNA was extracted from cells by using RNeasy® reagent (QIAGEN) according to the manufacturer's instructions. cDNA synthesis and amplification via PCR were performed using Transcriptor High Fidelity cDNA Synthesis Kit (Roche Diagnostics GmbH, Mannheim, Germany). The cDNA was used for PCR by LightCycler® FastStart DNA Master PLUS SYBR Green I (Roche). The PCR reaction mixture was made up in 20 μL of 10 μM targeted gene oligonucleotides primers. Using LightCycler® (Roche), heat denaturation at 95 °C for 10 min and 40 cycles of PCR

Table 1
Primer sequences used for real-time RT-PCR.

Gene	Accession	Sense primer	Antisense primer
ALP	NM_007431	GTTGCCAAGCTGGGAGAACAC	CCCACCCCGCTATTCCAAAC
β-Actin	NM_007393	TATGGAATCCTGTGGCATCC	CTTCTGCATCCTGTCAGCAA

with denaturing at 95 °C for 10 s, annealing temperature 55 °C for 10 s and extension at 72 °C for 10 s were performed ALP and β-Actin. The sequences of all primers are shown in detail in Table 1.

2.12. In vivo fluorescent imaging of ASCs labeled with QDs

QDs655, QDs755 or QDs800 were transduced into ASCs using R8 in the same way. ASCs (0.5, 1 and 3 × 10^5 cells) labeled with QDs were subcutaneously transplanted with 50 μL PBS into the back of C57BL/6 mice. Images were taken using the Maestro *in vivo* imaging system (CRI Inc, Woburn, MA; excitation filter: 575–605 nm, emission filter: 645 nm long pass). The detection was set to capture images automatically at 10-nm increments from 630 nm to 850 nm with constant 1 s exposure. The resulting TIFF images were loaded into the vendor's software and analyzed.

On the other hand, for the *in vivo* imaging of ASCs transplanted into mouse through the tail vain, ASCs (5 × 10^5 cells) labeled with QDs800 were injected with 0.15 mL saline. Images were taken using the Maestro *in vivo* imaging system in the same way after 10 min. Moreover, for the histological analysis, ASCs (5 × 10^5 cells) labeled with QDs655 were injected into the mouse. The mouse was then sacrificed after 10 min and major organs (heart, lung, liver, spleen and kidney) were harvested and washed three times with PBS to remove retained erythrocytes. The collected tissue specimens were then fixed by formalin and embedded in paraffin. To examine the histological QDs uptake and distribution of transplanted ASCs, the tissue specimens were cut into 10 μm thick sections and then were observed by fluorescent microscopy.

2.13. Statistical analysis

Numerical values are presented as the mean ± SD. Each experiment was repeated three times. Statistical significance was evaluated using unpaired Student's *t*-test for comparisons between the two groups; *p*-values < 0.05 were considered to be statistically significant. All statistical analyses were performed using the SPSS software package.

3. Results

3.1. Transduction of QDs into ASCs using R8

QDs655 (2.0 nM) were mixed with concentrations of R8 (0, 0.2, 2.0, 20 and 200 μM) for 20 min respectively and they were tested for their ability to transduce into ASCs using conventional fluorescent microscopy and flow cytometry analysis. Red fluorescence derived from QDs655 was strongly observed at the ratio of 20 μM R8 to 2.0 nM QDs655. Increasing the R8 peptide concentration beyond 20 μM did not increase the QDs655 internalization. This result suggests that the concentration ratio of QDs:R8 of 1:1 × 10^4 is optimal for delivery into ASCs (Fig. 1A).

3.2. Cytotoxicity to ASCs

QDs655 was transduced into ASCs using R8 at various concentrations in transduction medium for 24 h at 37 °C. Significant cytotoxicity was observed in ASCs transduced with more than

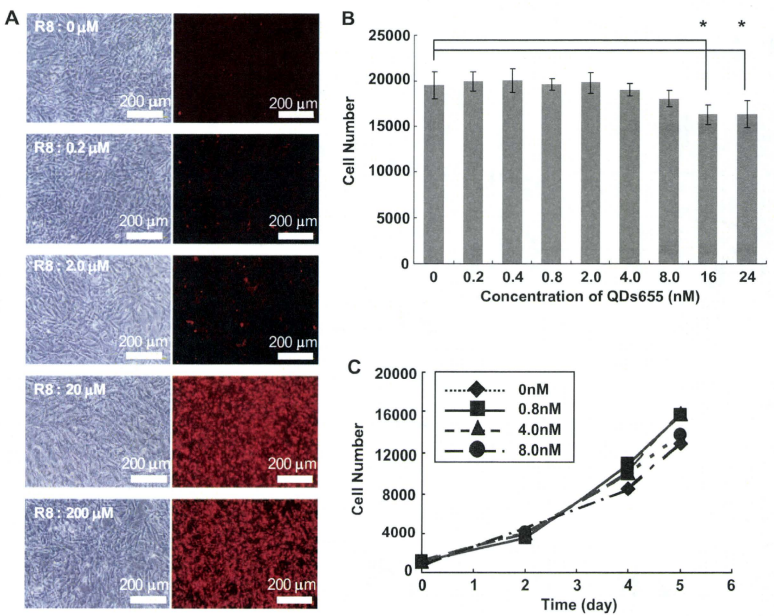

Fig. 1. Optimal formation of R8-QDs and the cytotoxicity to ASCs. A: QDs655 (2.0 nM) were mixed with various concentrations of R8 for 20 min and the complex were transduced into ASCs for 4 h to determine the optimal concentration ratio of QDs/R8. B: ASCs were transduced with QDs655 using R8 at various concentrations for 24 h. The survival of ASCs transduced with QDs655 using R8 is compared with non-transduction ASCs. C: The proliferation rate is shown in the nontoxic range of QDs655. The number of cells was estimated at 0, 2, 4, and 5 days after transduction as described in Materials and Methods. The data, all in triplicate, are shown as the mean ± SD values. *$p < 0.05$.

16 nM of QDs655, however, >80% of the cells were still alive. In addition, no remarkable cytotoxicity was observed with less than 8.0 nM of QDs655 (Fig. 1B). The morphology and fluorescent images were confirmed by conventional fluorescent microscopy.

Moreover, the influence on the proliferation rate was examined within the non-cytotoxic range of concentrations. The cells were confirmed to exhibit a logarithmic growth rate that was nearly equal to normal ASCs. There were no significant differences in these concentrations (Fig. 1C). These data suggest that ASCs could be labeled within an 8.0 nM concentration of QDs using R8.

3.3. Transduction efficiency of QDs using R8

To determine the transduction efficiency of QDs into ASCs, ASCs were transduced with QDs655 using R8 for 1 h at 0, 0.8, 2.0 and 8.0 nM concentrations of QDs655. The internalization of QDs655 was estimated and compared using flow cytometry analysis. The transduction efficiency of QDs655 after 1 h transduction was 81.4 ± 5.4% at 0.8 nM, 90.8 ± 2.8% at 2.0 nM and 95.2 ± 1.9% at 8.0 nM (Fig. 2A). More than 80% of the cells could be labeled within 1 h (Fig. 2B).

In addition, the location and fluorescent intensity of QDs655 was analyzed using confocal laser scanning microscopy at a concentration of 0.4 nM QDs655 after 1 h of transduction. The successive location of QDs655 in the ASCs was observed in 1 h, 8 h, 1 day, 7 days, 10 days and 14 days after transduction. QDs655 were widely dispersed in the cell cytoplasm during the early time points, however, aggregation of QDs655 was observed as time passed. QDs655 could not be observed in the nuclei at any time (Fig. 3A). The fluorescent intensity level of QDs655 was approximately equal during 14 days (Fig. 3B).

3.4. Transduction of QDs using R8 by macropinocytosis

The internalization of QDs655 using R8 with sodium azide and 2-deoxy-D-glucose, or amiloride, or at 4 °C was compared to that of normal transduction. The fluorescence of QDs655 could be observed on the face of the ASCs only and not in the cytoplasm (Fig. 4A–C). On the other hand, QDs655 were incorporated into the cytoplasm of ASCs after no application of inhibitors (Fig. 4D). These results suggested that the internalization of QDs655 using R8 occurs mainly by macropinocytosis.

3.5. Differentiation of ASCs transduced with QDs using R8

To examine the influence on the pluripotency of ASCs, ASCs were transduced with 0.4 nM of QDs655 using R8 and cultured with adipogenic and osteogenic medium for 2 weeks. Following adipogenic differentiation, intracellular lipid droplets in ASCs labeled with QDs655 were observed in the same frequency as the control ASCs and the red fluorescence derived from internalized QDs655 was confirmed (Fig. 5A-a). Oil Red O staining confirmed that intracellular droplets were lipid (data not shown). On the other hand, after incubation in osteogenic medium, ASCs labeled with QDs655 became osteocyte-like in morphology with cuboidal shapes (Fig. 5A-b). The cells were positive for von Kossa's staining in the same frequency as the control ASCs (data not shown). Red fluorescence of QDs655 was clearly observed for more than 2 weeks using confocal laser scanning microscopy in both of the differentiated cell types. However, the fluorescence of QDs655 was only slightly observed in the ASCs cultured with normal culture medium (Fig. 5A-c).

Moreover, to estimate the influence on osteogenic differentiation ability of ASCs at the mRNA revel, ALP activity was measured by real-time RT-PCR. ALP activity of ASCs transduced with QDs655

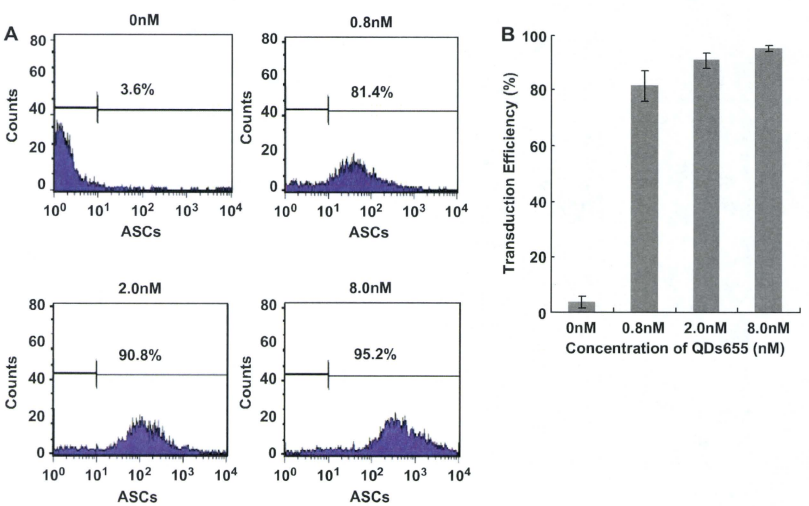

Fig. 2. Transduction efficiency of QDs using R8 quantified by flow cytometry. A: The transduction efficiency of QDs655 into ASCs using R8 after 1 h of incubation was quantified by flow cytometry. The mean fluorescent units are the average of 10,000 units. B: The bar graph shows the transduction efficiency of QDs655 using R8 after 1 h of transduction.

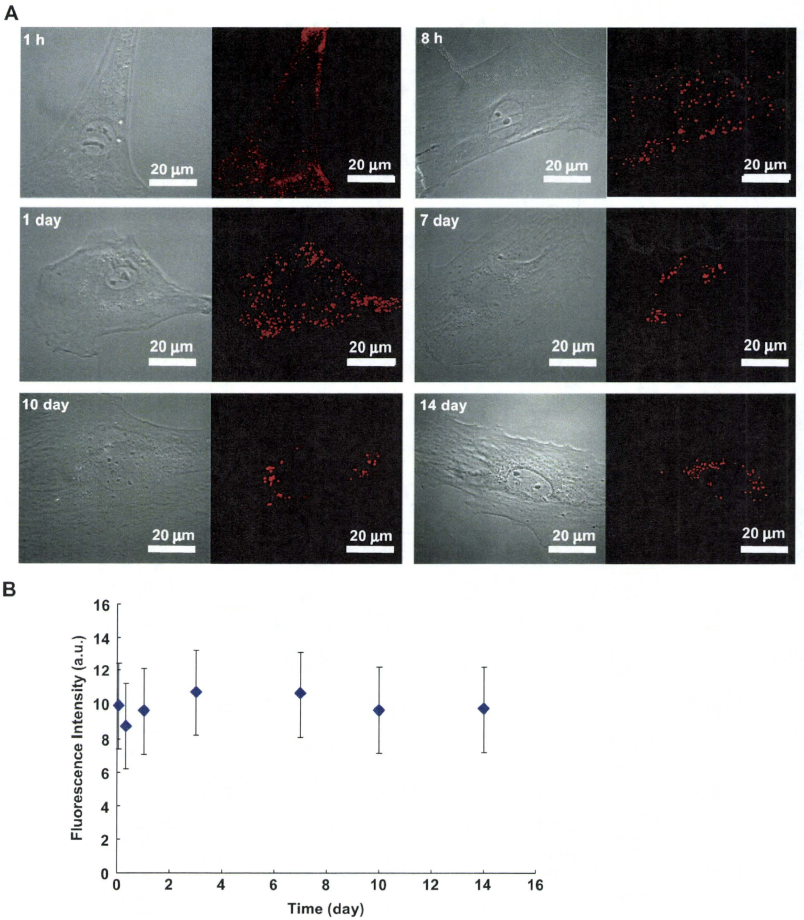

Fig. 3. Intracellular distribution and fluorescence intensity of QDs. A: The intracellular distribution of QDs655 in 1 h, 8 h, 1 day, 7 days, 10 days and 14 days after transduction were obtained by confocal laser scanning microscopy. Internalized QDs655 are shown by the red fluorescence. B: The fluorescence intensity was measured by confocal laser scanning microscopy. The data, in each triplicate, are shown as the mean ± SD values.

using R8 in osteogenic differentiation was observed at the same level as that of the non-transduced ASCs (Fig. 5B and C). These data suggested that the differentiation ability of ASCs was not inhibited by QDs655 transduction using R8.

3.6. Detection sensitivity for in vivo imaging

ASCs (0.5×10^5, 1.0×10^5 and 3.0×10^5 cells) labeled with QDs655 using R8 were injected subcutaneously with saline into the back of the mice. The Maestro Optical Imaging System (excitation filter: 575–605 nm, emission filter: 645 nm long pass) was used to observe the mice 1 h after transplantation. Moreover, images were obtained 1, 2, 5 and 7 days after transplantation (Fig. 6A) and the intensity was evaluated (Fig. 6B). The results suggested that ASCs labeled with QDs655 could be detected up to 7 days following subcutaneous transplantation.

On the other hand, one of the advantages of QDs is their ability for multiplex imaging. Multiplex imaging may be applied for

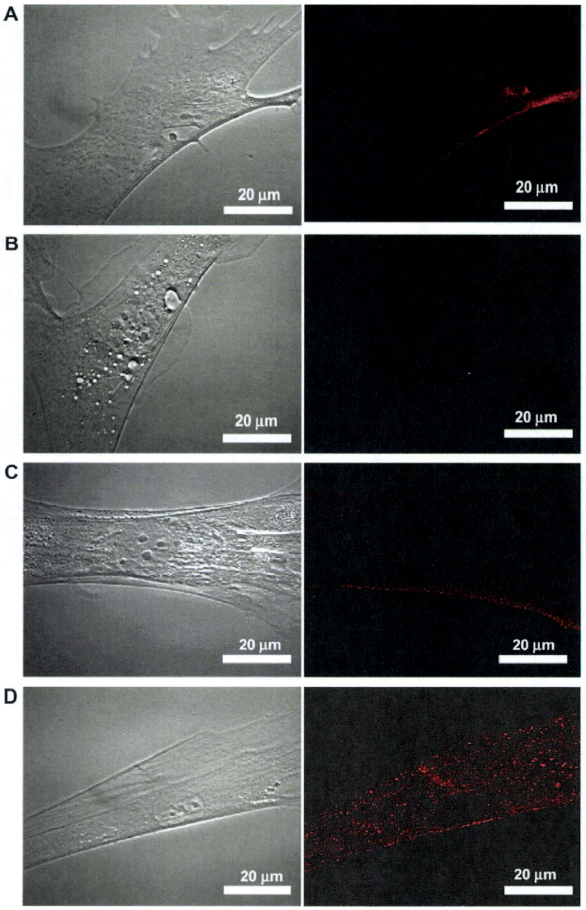

Fig. 4. Transduction mechanism of QDs using R8 into ASCs. A: ASCs were preincubated in the transduction medium with 10 mM sodium azide and 2-deoxy-D-glucose (endocytosis inhibitors) for 1 h at 37 °C. B: ASCs were preincubated in the transduction medium with 3 mM amiloride (macropinocytosis inhibitor) for 10 min at 37 °C. C: ASCs were preincubated in the transduction medium for 30 min at 4 °C (both endocytosis and macropinocytosis inhibitors). These cells were washed three times with PBS followed by addition of 0.4 nM QDs655 using R8 in the fresh transduction medium for 1 h. D: ASCs were incubated with 0.4 nM QDs655 with R8 under the normal transduction condition. These cells were observed using confocal laser scanning microscopy.

tracing different cell populations at the same time. Almost all kinds of QDs can be excited by the same wavelength and a different wavelength of light is emitted depending on the size of the QDs. In this study, ASCs (1×10^5 cells) were labeled with QDs655, 705 and 800 using R8 respectively and subcutaneously transplanted into the back of the mice and the multiplex image in 1 h was obtained in 1 h after transplantation (Fig. 6C).

Furthermore, ASCs labeled with QDs800 using R8 were transplanted through the tail vein of a mouse to examine whether the fluorescence of QDs800 from the ASCs could be detected and demonstrate the distribution of transplanted ASCs. When the mouse was sacrifice after 10 min, the fluorescence of QDs800 could be detected in the lung only by the Maestro *in vivo* imaging system (Fig. 7A). On the other hand, a histological analysis showed that the

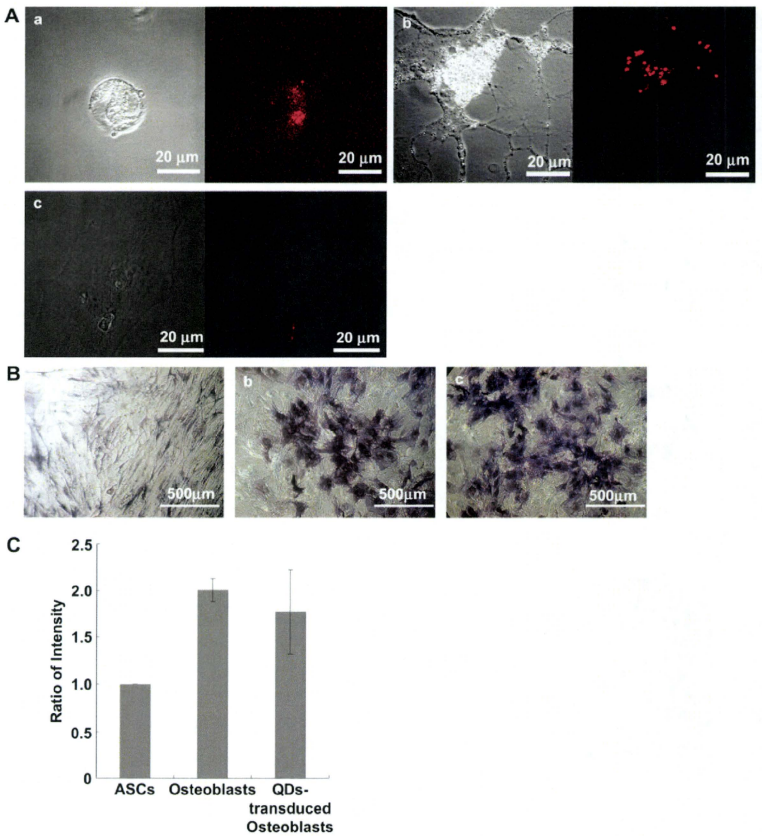

Fig. 5. Differentiation of ASCs transduced with QDs using R8. A: ASCs transduced with QDs655 (0.4 nM) using R8 were differentiated to lipocytes (a) or osteocytes (b) for 2 weeks. ASCs transduced with QDs655 (0.4 nM) using R8 were incubated in the culture medium without differentiation (c). These figures were obtained using confocal laser scanning microscopy. Phase contrast (left) and QDs655 fluorescent (right) were shown. B: Negative ALP staining of normal cultured (non-differentiated) ASCs (a), positive ALP staining of osteogenic induced ASCs (b) and osteogenic induced ASCs transduced with QDs655 using R8 (c) were confirmed. C: The quantification of ALP mRNA levels was compared in three groups. There was no significant difference between non-transduced ASCs and ASCs transduced with QDs655 using R8 ($p > 0.05$), but significantly more ALP activity was expressed than in the control ASCs ($p < 0.05$).

presence of ASCs could be confirmed in slices of the lungs only using conventional fluorescent microscopy (Fig. 7C). The heart and kidney data were not shown.

4. Discussion

Several studies have reported that some cells could passively internalize QDs in the culture medium without carrier or microinjection, electroporation and liposome-based transduction [7,11]. ASCs could not be transduced with QDs only without the help of carriers (data not shown). A cationic liposome "Lipofectamine" was used for the transduction of QDs into ASCs without further modification [17]. However, cytotoxicity was observed at a comparatively low concentration of >2.0 nM. In addition, the transduction time was relatively long (4 h at 0.8 nM of QDs655). Recently, CPPs mediated transduction has attracted more and more attention for the efficient cellular membrane delivery and labeling [12,20,21].

R8 which exhibits even greater efficiency in the delivery of several proteins was employed in order to overcome these problems. Moreover, compared with other articles [4,7,8], the transduction efficiency of R8 seems to be similar to CLO-Tat, CHPNH2 and pep-1. On the other hand, the molecular length of R8 is shorter

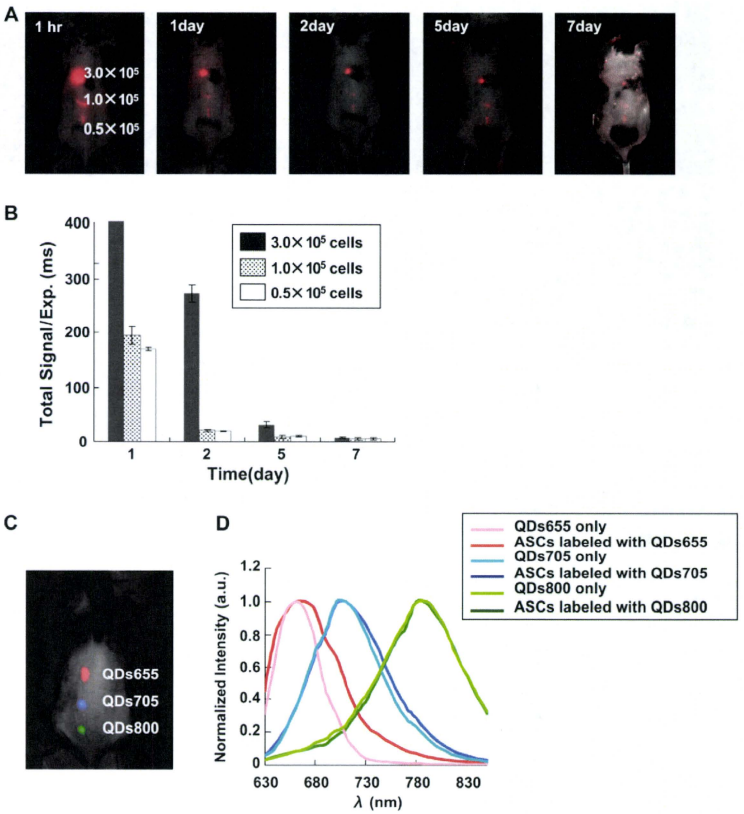

Fig. 6. Detection and multiplex imaging capability of QDs in subcutaneous transplantation. A: ASCs (0.5×10^5, 1.0×10^5 and 3.0×10^5 cells) labeled with QDs655 (0.8 nM) using R8 were subcutaneously transplanted into the backs of the mice. These images were taken 1 h, 1, 2, 5 and 7 days past injection (excitation filter 575–605 nm, emission filter 645 nm long pass). B: The bar graph shows the change of fluorescence intensity of QDs655 for 7 days at the number of ASCs labeled with QDs655. C: ASCs (1.0×10^5 cells) labeled with QDs655, 705 and 800 were subcutaneously injected on the back of the mice. The image was taken 10 min after transplantation with a single excitation light source. D: The graph was the fluorescent spectra of ASCs labeled with QDs655, QDs705 and QDs800.

than the others, thus the cost of synthesis is lower than the others. The cytotoxicity was greatly reduced by using R8. No cytotoxicity was observed in ASCs transduced with less than 16 nM of QDs655, and no drastic decrease in the number of cells was observed with more than 8.0 nM of QDs655. These results suggested that the effect of internalized QDs on the cell cytotoxicity was dependent on surface coating rather than on the total amount of internalized QDs. Furthermore, as observed in a previous report, the current results indicate that ASCs labeled with QDs using R8 had no adverse effects on cell proliferation, measured by the CCK-8 assay [7]. On the other hand, the QDs transduction mechanism using R8 into ASCs was investigated by incubation at 4 °C, with inhibitors of endocytosis, such as sodium azide, and macropinocytosis, such as amiloride (Fig. 4). The QDs internalization was suppressed by these inhibitors, thus suggesting that the transduction of QDs into ASCs occurred through macropinocytosis.

The transduction time and maintenance of stem cell potency after transduction of QDs are very important, when QDs are employed clinically for regenerative medicine. In this study, the fluorescence intensity of internalized QDs reached almost its peak by 1 h. The transduction time of QDs using R8 was markedly decreased in comparison to Lipofectamine [17]. On the other hand, the CPPs delivery of QDs rescued the cells from the negative effects caused by the internalized QDs to osteogenic and chondrogenic-associated lineage markers [7]. ASCs transduced with QDs655 using R8 cultured with adipogenic and osteogenic

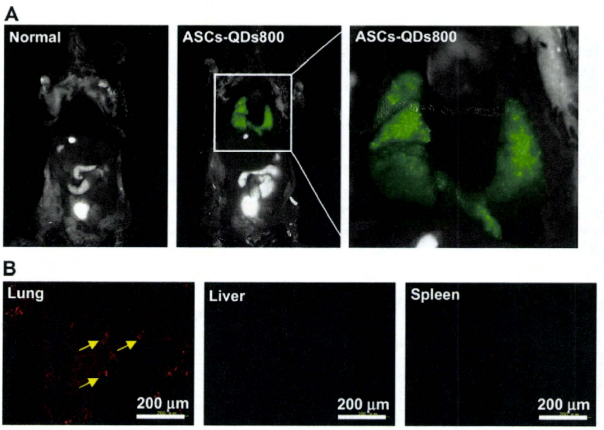

Fig. 7. *In vivo* imaging of ASCs labeled with QDs after intravenous injection. A: ASCs (5.0×10^5 cells) labeled with QDs800 (0.8 nM) using R8 were transplanted through the tail vain into mouse. The images were taken 10 min after injection (excitation filter 575–605 nm, emission filter 645 nm long pass). B: The red fluorescence of QDs655 was detected in the lung only, with little or no QDs655 accumulation in the liver or spleen.

medium for 2 weeks differentiated into adipogenic and osteogenic cells, respectively, in the current study. ALP activity of ASCs transduced with QDs655 using R8 following osteogenic differentiation was exhibited at the same level as that for the non-transduced ASCs. Moreover, Jui-Chih Chang et al. checked the influence to the cell surface of ASCs with QDs using cell-penetrating peptide (CPP). In mesenchymal stem cells (MSCs), cell surface receptors such as CD29, CD44, CD73, CD90, CD105, etc. are accredited the prototypical markers. According to the reference, it was found that CPP delivery preserved CD29, CD44, CD73, CD90 and CD105 expressions [7]. These data suggested that ASCs transduced with QDs using R8 maintained their stem cell potency. However, Jui-Chih Chang et al. reported that Pep-1, a CPP, coated QDs, affected the gap junctions of human mesenchymal stem cell [13]. It will be necessary to ascertain the influence of R8 on gap junctions of ASCs in future studies. The fluorescence intensity in differentiated ASCs transduced with QDs655 was sustained at least for 2 weeks. On the other hand, undifferentiated ASCs transduced with QDs655 in the culture medium, showed markedly reduced fluorescence intensity after 2 weeks of culture. The differences may be due to their proliferative activity [5]. However, the QDs655 signal was confirmed, thus suggesting that QDs could be available for labeling of ASCs for 2 weeks.

QDs exhibit several advantages in comparison to conventional organic labels, such as a high luminance, resistance to photobleaching, a range of excitation wavelengths and narrow emission bandwidths. Therefore, QDs have a potential application for *in vivo* imaging. ASCs labeled with QDs655 using R8 were subcutaneously injected with saline into the backs of the mice. ASCs labeled with QDs655 could be detected up to 7 days following subcutaneous transplantation, but the fluorescence intensities were drastically decreased. This reduction might be due to the rapid division of ASCs as suggested in a previous report [22]. When the ASCs labeled with QDs655 were incubated with DMEM/F12 mediun containing 2% FBS, the fluorescence of QDs was maintained for 2 weeks at almost the same label. This result was suggested that internalized QDs were diluted by cell proliferation in the culture medium and incorporated into the cytoplasm of ASCs after escape from the lysosome fraction system [23]. Another advantage of QDs is their ability to for multiplex imaging of different QDs at the same time [22]. When ASCs transduced with QDs655, 705 and 800 respectively were transplanted into the back of mouse subcutaneously at the different points, their fluorescence of all three species could be observed at the same time 1 h after transplantation.

On the other hand, QDs fluorescence below the wavelength range 650 nm was not used often for sensitive imaging of deeper tissues in recent papers [22,24,25]. Deep tissue imaging (millimeters to centimeters) requires the use of far red and near infrared light in the spectral range 650–900 nm [26], because these regions eliminated overlap with major absorption peaks of blood and water *in vivo*. When ASCs labeled with QDs800 were transplanted through the tail vein into a mouse, the fluorescence could be detected in the lung. ASCs labeled with QDs655 and 705 could not be observed *in vivo* because of the strong autofluorescence of liver tissue. Besides, it was reported that QDs fluorescence could be detected in other organs such as the liver and spleen in other papers [12]. In this study, mice were killed 10 min after ASCs transplantation and this suggested that almost all ASCs stayed in the lung. Therefore, i.v. ASCs transplantation may be useful treatment modality for lung disease in the future [24].

As for the fate of QDs using R8 *in vivo*, Neera V. Gopee et al. showed that when QDs were injected intradermally (ID) on the right dorsal flank of the female SFH-1 hairless mice, the QDs could be observed moving from the injection sites apparently through the lymphatic duct system to regional lymph nodes within minutes. Residual QDs remained at the site of injection until necropsy at 24 h. Moreover, using inductivity coupled plasma mass spectrometry (ICP-MS), showed accumulation in the liver, regional draining lymph nodes, kidney, spleen, and hepatic lymph node [27].

On the other hand, Hak Soo Choi et al. showed that when QDs leaked into the vascular in the intravenously injection, the QDs were accumulated in the liver. And then, the QDs were transported to the kidney and cleared by urinary excretion [28].

5. Conclusion

ASCs possess the ability of self-renewing and differentiating into various mesenchymal cell types. Because of their potential clinical application, it has therefore become important to label the cells for tracing as transplanted cells. The concentration ratio of QDs:R8 of $1:1 \times 10^4$ was optimal for delivery into ASCs and the cells could be labeled within an 8.0 nM concentration of QDs using R8. In addition, ASCs could be labeled within about 1 h and the fluorescent intensity level of QDs was during 14 days at least. The differentiation ability of ASCs was not inhibited by QDs transduction using R8. Moreover, ASCs labeled with QDs could be detected following subcutaneous transplantation and injection through tail vein *in vivo*. This study suggested that QDs labeling using R8 could be utilized for the imaging of ASCs.

Acknowledgements

This work was supported by the Kobayashi Pharmaceutical Company. We thank Miwa Natsume, Takafumi Kinoshita and Rio Fujita for technical advice, and Yukiko Masuda, Nagisa Otake and Sumiko Nishio (Nagoya University) for their assistance.

Appendix

Figures with essential color discrimination. All figures of this article are difficult to interpret in black and white. The full color images can be found in the on-line version, at doi:10.1016/j.biomaterials.2010.01.134.

References

[1] Seleverstov O, Zabirnyk O, Zscharnack M, Bulavina L, Nowicki M, Heinrich JM, et al. Quantum dots for human mesenchymal stem cells labeling. A size-dependent autophagy activation. Nano Lett 2006;6(12):2826–32.
[2] Zhang T, Stilwell JL, Gerion D, Ding L, Elboudwarej O, Cooke PA, et al. Cellular effect of high doses of silica-coated quantum dot profiled with high throughput gene expression analysis and high content cellomics measurements. Nano Lett 2006;6(4):800–8.
[3] Zhang Y, He J, Wang PN, Chen JY, Lu ZJ, Lu DR, et al. Time-dependent photoluminescence blue shift of the quantum dots in living cells: effect of oxidation by singlet oxygen. J Am Chem Soc 2006;128(41):13396–401.
[4] Hsieh SC, Wang FF, Lin CS, Chen YJ, Hung SC, Wang YJ. The inhibition of osteogenesis with human bone marrow mesenchymal stem cells by CdSe/ZnS quantum dot labels. Biomaterials 2006;27(8):1656–64.
[5] Hoshino A, Hanaki K, Suzuki K, Yamamoto K. Applications of T-lymphoma labeled with fluorescent quantum dots to cell tracing markers in mouse body. Biochem Biophys Res Commun 2004;314(1):46–53.
[6] Jaiswal JK, Mattoussi H, Mauro JM, Simon SM. Long-term multiple color imaging of live cells using quantum dot bioconjugates. Nat Biotechnol 2003;21(1):47–51.
[7] Chang JC, Su HL, Hsu SH. The use of peptide-delivery to protect human adipose-derived adult stem cells from damage caused by the internalization of quantum dots. Biomaterials 2008;29(7):925–36.
[8] Ohyabu Y, Kaul Z, Yoshioka T, Inoue K, Sakai S, Mishima H, et al. Stable and nondisruptive *in vitro*/*in vivo* labeling of mesenchymal stem cells by internalizing quantum dots. Hum Gene Ther 2009;20(3):217–24.
[9] Toita S, Hasegawa U, Koga H, Sekiya I, Muneta T, Akiyoshi K. Protein-conjugated quantum dots effectively delivered into living cells by a cationic nanogel. J Nanosci Nanotechnol 2008;8(5):2279–85.
[10] Shah B, Clark P, Stroscio M, Mao J. Labeling and imaging of human mesenchymal stem cells with quantum dot bioconjugates during proliferation and osteogenic differentiation in long term. Conf Proc IEEE Eng Med Biol Soc 2006;1:1470–3.
[11] Lagerholm BC. Peptide-mediated intracellular delivery of quantum dots. Methods Mol Biol 2007;374:105–12.
[12] Lei Y, Tang H, Yao L, Yu R, Feng M, Zou B. Applications of mesenchymal stem cells labeled with Tat peptide conjugated quantum dots to cell tracking in mouse body. Bioconjug Chem 2008;19(2):421–7.
[13] Chang JC, Hsu SH, Su HL. The regulation of the gap junction of human mesenchymal stem cells through the internalization of quantum dots. Biomaterials 2009;30(10):1937–46.
[14] Shah BS, Clark PA, Moioli EK, Stroscio MA, Mao JJ. Labeling of mesenchymal stem cells by bioconjugated quantum dots. Nano Lett 2007;7(10):3071–9.
[15] Yukawa H, Noguchi H, Oishi K, Miyazaki T, Kitagawa Y, Inoue M, et al. Recombinant sendai virus-mediated gene transfer to adipose tissue-derived stem cells (ASCs). Cell Transplant 2008;17(1–2):43–50.
[16] Yukawa H, Noguchi H, Oishi K, Takagi S, Hamaguchi M, Hamajima N, et al. Cell transplantation of adipose tissue-derived stem cells in combination with heparin attenuated acute liver failure in mice. Cell Transplant 2009;18(5):601–9.
[17] Yukawa H, Mizufune S, Mamori C, Kagami Y, Oishi K, Kaji N, et al. Quantum dots for labeling adipose tissue-derived stem cells. Cell Transplant 2009;18(5):591–9.
[18] Mattheakis LC, Dias JM, Choi YJ, Gong J, Bruchez MP, Liu J, et al. Optical coding of mammalian cells using semiconductor quantum dots. Anal Biochem 2004;327(2):200–8.
[19] Akita H, Ito R, Khalil IA, Futaki S, Harashima H. Quantitative three-dimensional analysis of the intracellular trafficking of plasmid DNA transfected by a nonviral gene delivery system using confocal laser scanning microscopy. Mol Ther 2004;9(3):443–51.
[20] Zhao M, Kircher MF, Josephson L, Weissleder R. Differential conjugation of tat peptide to superparamagnetic nanoparticles and its effect on cellular uptake. Bioconjug Chem 2002;13(4):840–4.
[21] Lewin M, Carlesso N, Tung CH, Tang XW, Cory D, Scadden DT, et al. Tat peptide-derivatized magnetic nanoparticles allow *in vivo* tracking and recovery of progenitor cells. Nat Biotechnol 2000;18(4):410–4.
[22] Lin S, Xie X, Patel MR, Yang YH, Li Z, Cao F, et al. Quantum dot imaging for embryonic stem cells. BMC Biotechnol 2007;7:67.
[23] Mudhakir D, Akita H, Khalil IA, Futaki S, Harashima H. Pharmacokinetic analysis of the tissue distribution of octa-arginine modified liposomes in mice. Drug Metab Pharmacokinet 2005;20(4):275–81.
[24] Suzuki H, Hogg JC, van Eeden SF. Sequestration and homing of bone marrow-derived lineage negative progenitor cells in the lung during pneumococcal pneumonia. Respir Res 2008;9:25.
[25] So MK, Xu C, Loening AM, Gambhir SS, Rao J. Self-illuminating quantum dot conjugates for *in vivo* imaging. Nat Biotechnol 2006;24(3):339–43.
[26] Gao X, Cui Y, Levenson RM, Chung LW, Nie S. *In vivo* cancer targeting and imaging with semiconductor quantum dots. Nat Biotechnol 2004;22(8):969–76.
[27] Gopee NV, Roberts DW, Webb P, Cozart CR, Siitonen PH, Warbritton AR, et al. Migration of intradermally injected quantum dots to sentinel organs in mice. Toxicol Sci 2007;98(1):249–57.
[28] Choi HS, Liu W, Misra P, Tanaka E, Zimmer JP, Itty Ipe B, et al. Renal clearance of quantum dots. Nat Biotechnol 2007;10:1165–70.